JOURNAL OF CATALYSIS 133, 28–41 (1992)

The Synthesis and Cracking Behavior of Zeolite-Amorphous Silica–Alumina Composites Prepared Using Gels with High Alumina and Low Organic Template Content

PRASAD YARLAGADDA, CARL R. F. LUND, AND ELI RUCKENSTEIN[1]

Department of Chemical Engineering, State University of New York at Buffalo, Amherst, New York 14260

Received March 25, 1991; revised July 16, 1991

Composites of ZSM-5 and amorphous silica–alumina have been prepared from starting gels with SiO_2/Al_2O_3 molar ratios of 10 and below and tetrapropyl ammonium $(TPA^+)/Al_2O_3$ molar ratios below 0.5. The syntheses have been followed by periodic removal of aliquots from the gel with subsequent analysis. At $SiO_2/Al_2O_3 = 10$ and $TPA^+/Al_2O_3 = 0.44$ mordenite formed. When the SiO_2/Al_2O_3 ratio was reduced to 8.3, but the ratio TPA^+/Al_2O_3 was kept at 0.45, crystallization progressed from the initial formation of P_c to a mixture of P_c plus ZSM-5 to finally only ZSM-5 at the end of the run. At the lower SiO_2/Al_2O_3 ratio of 6 the P_c phase persisted, in a mixture with ZSM-5, until the end of the run. At the lowest SiO_2/Al_2O_3 ratio employed, 3.5, only P_c was detected for a TPA^+/Al_2O_3 ratio of 0.4. In all cases an amorphous silica–alumina coexisted with the zeolites. Samples removed periodically from gels having initial molar ratios of $SiO_2/Al_2O_3 = 8.3$ and $TPA^+/Al_2O_3 = 0.45$ were calcined and subsequently converted to the H^+ form of ZSM-5 and evaluated in the cracking of *n*-hexane. These catalysts, which contained between 10 and 42 wt% HAlZSM-5 were more active than either pure HAlZSM-5 or mechanical mixtures prepared by the addition of preformed ZSM-5 powder (from 10 to 42 wt%) to an amorphous silica–alumina gel. All catalysts examined did show comparable selectivity to C_6–C_{10} aromatics when compared at equal conversions. Both types of catalysts, namely those crystallized *in situ* and those prepared mechanically, had comparable numbers of strong acid sites (relative to the amount of HAlZSM-5) as measured by the temperature-programmed desorption of ammonia. The better connectivity between the two phases is suggested to be responsible for the greater activity of the composites in which the ZSM-5 crystallizes *in situ*, compared to the mechanical mixtures.

INTRODUCTION

Jacobs *et al.* (*1*) have observed that by interrupting the synthesis of ZSM-5 during its preparation from a gel of composition 125 TPAOH–Na_2O–Al_2O_3–200 SiO_2–5500 H_2O, a solid that is amorphous to X-rays but has IR framework vibrations and shape selectivity characteristics of crystalline ZSM-5 is obtained. They suggested that this solid consisted of submicrocrystalline ZSM-5 nuclei with sizes well below the threshold limit of X-ray detection dispersed in an amorphous matrix. The catalytic activity of this material in the hydrocracking of *n*-decane, while much smaller than the activity of pure ZSM-5, was due mainly to the zeolite fraction. The amorphous matrix of the catalyst was predominantly silica and therefore is not expected to have catalytic activity since it has no acidic sites. However, it could still affect the activity and/or selectivity of the composite via diffusion (*2, 3*). Such an effect is due to the higher rate of diffusion in the larger pores of the matrix than that in the pores (5–6 Å) of the zeolite.

More complex behavior is expected to occur when the matrix also possesses active sites. In order to prepare such a catalyst in a manner analogous to that of Jacobs *et al.* (*1*), a high alumina content is necessary in the starting gel. Then a fraction of the alu-

[1] To whom correspondence should be addressed.

0021-9517/92 $3.00

mina can be incorporated in the zeolitic framework, and the remaining part, along with the unconverted silica, can form an amorphous aluminosilicate matrix that contains acidic sites. The first objective of the present study was to synthesize a composite catalyst that contains a highly siliceous zeolite, such as ZSM-5, and an alumina-rich amorphous silica–alumina matrix. It has been found that there are conditions under which a ZSM-5 phase can be crystallized *in situ* from an alumina-rich gel at low TPA^+ content. The second objective was to compare the activity and selectivity of the composite catalyst to those of pure ZSM-5 and to corresponding samples prepared by dispersing preformed ZSM-5 in an alumina–silica gel.

As noted in numerous papers (*4–6*), the formation of the ZSM-5 phase depends on the SiO_2/Al_2O_3, TPA^+/SiO_2, and $(Na^+ + TPA^+)/Na^+$ ratios, as well as the duration and temperature of synthesis. Synthesis in the absence of organic additives (*7, 8*) has revealed that for SiO_2/Al_2O_3 molar ratios <30 in the gel, the mordenite phase forms predominantly. Only in the very narrow range of molar ratios between 40 and 45 is the ZSM-5 phase formed, albeit at a molar ratio Na_2O/Al_2O_3 of 4.5. However, the presence of organic additives such as tetrapropyl ammonium cations (TPA^+) permits the formation of the ZSM-5 phase from starting gels with a very wide range of SiO_2/Al_2O_3 molar ratios (20–100) (*9, 10*). It has also been noted that an optimum TPA^+/SiO_2 ratio must be used (*11*) in order to obtain highly crystalline ZSM-5.

Another important variable that determines the type of zeolite as well as its yield is the synthesis temperature. Temperatures greater than 100°C decrease the induction time (*11*), a trend normally encountered in the synthesis of many zeolites. Both Barrer (*12*) and Breck (*13*) have presented a detailed discussion regarding the low-temperature zeolite formation. Starting from a gel mixture containing the following four components, $Na_2O–Al_2O_3–SiO_2–H_2O$, and using temperatures in the range of 60–100°C, the Zeolites A, P, X, Y, R, and S can be synthesized. The inclusion of a quaternary alkyl ammonium compound (TPA^+, TMA^+) in the gel leads to additional types of zeolites including the more siliceous ones, like ZSM-5 and ZSM-11.

In spite of the wealth of information available regarding various aspects of the synthesis of the pentasil family of high-silica zeolites starting from gels rich in silica and in organic template, no information is available for alumina-rich gels of low organic content. The present investigation is focused on synthesis using starting gels having (i) SiO_2/Al_2O_3 molar ratios of 10 or less; (ii) $TPA/Al_2O_3 < 0.5$, and (iii) a synthesis temperature of less than 100°C. The first condition was chosen in order to have 10–15 wt% Al_2O_3 in the amorphous phase and thus to generate acidic sites. The second condition ensures that only a part of the silica–alumina from the gel converts to the ZSM-5 phase. The progress of crystallization and the identification and quantification of the phases formed have been carried out using X-ray powder diffraction, supplemented with FT–IR investigations.

The catalytic activity and selectivity of the above type of composite catalysts in their protonated form were assessed using *n*-hexane cracking as a probe reaction. For comparison purposes, the *n*-hexane cracking was also carried out over catalysts prepared by dispersing preformed ZSM-5 in a silica–alumina gel, and also over pure ZSM-5 zeolite. Furthermore, the acidic characteristics of the composite catalysts of both types have been determined using the temperature-programmed desorption of adsorbed ammonia molecules.

EXPERIMENTAL

Gel Preparation and Synthesis

Technical sodium silicate aqueous solution (40–42° Bé, Fisher Scientific) containing 28.5 wt% SiO_2 and 7.7 wt% Na_2O was used as the silica source, and purified sodium aluminate (Fisher Scientific) con-

taining 43.5 wt% Al_2O_3 and 30.0 wt% Na_2O was used as the alumina source. The other chemicals employed were tetrapropyl ammonium bromide (Aldrich), sodium chloride (Fisher Scientific), and sulfuric acid (Fisher Scientific). A typical gel was obtained as follows: individual solutions containing the above chemicals in such quantities so as to obtain the required molar compositions were first prepared. These solutions were mixed under stirring for at least 15 min in a blender after which the pH was adjusted to 12 ± 0.5 followed by an additional 15 min of stirring. Subsequently, the gel was transferred to a 1-liter three-neck clean glass flask provided with a stirrer, water-cooled condenser, and a sampling port. The gel was heated under reflux at 95°C and stirred continuously. Samples from the slurry were withdrawn periodically and were immediately cooled to room temperature by the addition of distilled water followed by filtration, washing, and drying at 100 ± 5°C overnight. In some cases, when needed for sample characterization, additional heat treatment was conducted at 550 ± 10°C for 24 h in a muffle furnace in air.

X-Ray Diffraction and Infrared Studies

The various phases have been identified by X-ray diffraction with a STOE powder X-ray diffractometer that possesses a curved, position-sensitive detector and a Cu$K\alpha$ source of radiation. In order to quantify the amounts of the various phases, samples were finely mixed with 20 wt% MgO (99.6% purity, Baker analyzed) whose major reflection peak served as standard. The relative amounts of each of the phases present were evaluated as the ratio of the area under the selected reflection peak(s) ($2\theta = 23.2$ for ZSM-5; 28.2 for P_c; the arithmetic average corresponding to 9.8 and 26 for mordenite) to the area under the reflection peak $2\theta = 43.1$ of MgO after correcting each of the areas for the background. (For mordenite, the arithmetic average of the areas corresponding to the two intense peaks at $2\theta = 9.8$ and 26 was used for the calculation of the crystallinity to improve the quantitative determinations.)

For the determination of the absolute crystallinity of the samples, a calibration plot was constructed by using intimate physical mixtures containing 0–80 wt% pure ZSM-5 (Mobil, MZ-44), 80–0 wt% amorphous silica–alumina, and 20 wt% MgO.

The absorption infrared spectra were obtained with a Mattson Alpha Centauri Fourier transform-infrared spectrophotometer equipped with a data station in the mid-infrared (1400–400 cm^{-1}) range and having a resolution of 0.5 cm^{-1}. The thin wafers, used for recording the IR spectra, were prepared by employing the KBr pellet technique (1% wt sample in KBr).

Catalyst Preparation

The samples were prepared for use as catalysts by calcining in air at 550°C for 24 h, followed by ammonium ion exchange with 1 *M* $(NH_4)_2SO_4$ solution under reflux for 24 h, drying, and a final calcination at 550°C for 4 h.

Temperature-Programmed Desorption (TPD)

Temperature-programmed desorption (TPD) spectra of some of the catalyst samples using ammonia as the probe base molecule were recorded. The TPD setup and the experimental protocol were similar to those employed in our earlier work (*15*).

Catalyst Activity Measurements

The catalytic behavior of the composite catalysts prepared by *in situ* crystallization of ZSM-5, hereafter denoted as CA, was studied using *n*-hexane cracking as a probe reaction. The reaction was conducted in a plug-flow microreactor at atmospheric pressure. Purified helium at a predetermined flow rate was bubbled through an *n*-hexane saturator (at 20°C) before being passed into the reactor. In all the catalytic runs, 0.15 g of catalyst powder (particle size <150 μm) was used. The catalysts were pretreated by

heating at 500°C under helium flow for 1 h before starting the reaction. The exit gas stream was analyzed for C_1 to C_{20} hydrocarbons on a 10% SE-30 column equipped with a flame ionization detector. The reaction temperature was varied from 380 to 490°C, the space time from 0.2 to 1.5 (g catalyst)h/(g hexane), and the feed gas contained 5 mol% n-C_6H_{14} in helium. From the GC results, the n-hexane fractional conversion (x) and the C_6–C_{10} aromatic selectivity were calculated as follows:

$$\text{Conversion } (x) = \left(1 - \frac{\text{mol of } n\text{-}C_6H_{14} \text{ in the exit stream}}{\text{mol of } n\text{-}C_6H_{14} \text{ in the feed stream}}\right)$$

$$\text{Selectivity} = \left(\frac{\text{weight of } C_6\text{–}C_{10} \text{ aromatic fraction}}{\text{total weight of all hydrocarbons excluding exit } n\text{-hexane}}\right) \times 100.$$

For each of the catalysts tested, the rate constant (k) was obtained from the slope of the first-order plot of $-\ln(1 - x)$ against space time at a given reaction temperature. The activation energy E_a was calculated from an Arrhenius plot of $\ln k$ vs $1/T$.

The cracking of n-hexane was also studied using pure ZSM-5 and catalysts (hereafter denoted as CB) obtained by dispersing pure ZSM-5 particles in an amorphous silica–alumina gel. The pure zeolite was synthesized following the general procedure of Chen *et al.* but using different SiO_2/Al_2O_3 molar ratios than those given in their examples (*14*), while the CB type catalysts were made as described in our earlier work (*15*). Briefly, the procedure for preparing the CB composites involved the addition of a definite amount of preformed ZSM-5 zeolite powder to a solution containing sodium silicate and aluminum nitrate as soon as a turbidity due to the onset of gelation appeared in the solution. The pH was adjusted to 6.5–7.0. The zeolite content was varied from 10 to 45 wt%, whereas the Al_2O_3 content in the amorphous silica–alumina was kept at about 15 wt%.

RESULTS AND DISCUSSION

A. Preparation of Composites via in situ Crystallization

The molar compositions of the gels employed in the present study are summarized in Table 1. The crystallization temperature was maintained at 95°C during all these syntheses. The phases identified were mordenite, P_c and ZSM-5; they are listed in Table 1 in the order in which they were detected. The SiO_2/Al_2O_3 ratios of the starting gels and of the final composite powders for some samples are given in Table 2.

The SiO_2/Al_2O_3 molar ratio of the starting gel appears to be the main factor that determines the sequence in which the zeolite phases form as well as their yields. Thus, at a molar ratio of 10, and for both levels of TPA^+ template used (TPA^+/Al_2O_3 = 0.14 and 0.44), mordenite was the only crystalline phase detected (in addition to an amorphous phase); there was an induction period of 9–12 days before any crystalline material was detected. However, for comparable synthesis times, the crystallinity increased from 25 to 54 wt% when the TPA^+/Al_2O_3 molar ratio increased from 0.14 to 0.44. The induction period remained essentially unchanged.

For a starting SiO_2/Al_2O_3 molar ratio of 8.3, the zeolite P_c (also denoted B_1 in the literature) formed exclusively in the early stages of synthesis. Its amount increased with time, attained a maximum, and subsequently decreased to zero after 15 days of synthesis at 95°C. As the amount of P_c decreased, a concurrent increase in the amount of ZSM-5 was observed. As shown in Fig. 1, the maximum ZSM-5 XRD crystallinity was 42 wt%. The XRD patterns as a function of time for this batch are presented in Fig. 2. It should be noted that while the TPA^+/Al_2O_3 ratios were comparable for batches 2 and 3, the zeolite phases produced were completely different (mordenite for

TABLE 1

Gel Molar Composition

Batch no.	Composition (mol)					Zeolite phases (with increasing synthesis time)	Product composition of the final sample (wt%)	Duration of run (days)
	TPA Br	Na_2O	Al_2O_3	SiO_2	H_2O			
1	0.14	4.6	1	10.0	460	Mordenite (MOR)	25% MOR + 75% amorphous phase	15
2	0.44	4.8	1	10.0	440	Mordenite (MOR)	54% MOR + 46% amorphous phase	15
3	0.45	4.4	1	8.3	455	P_c, P_c + ZSM-5, ZSM-5	42% ZSM-5 + 58% amorphous phase	15
4	0.43	3.5	1	6.0	422	P_c, P_c + ZSM-5	26% P_c + 37% ZSM-5 + 37% amorphous phase	16
5	0.40	3.5	1	3.0	450	P_c	60% P_c + 40% amorphous phase	16
6	—	4.4	1	8.3	455	P_c	64% P_c + 36% amorphous phase	15
7[a]	0.45	4.4	1	8.3	455	P_c, P_c + ZSM-5	14% P_c + 32% ZSM-5 + 54% amorphous phase	17

Note. All the batches contained ~2 mol of NaCl per mol of Al_2O_3 in the starting gel.

[a] TPA Br solution was added to the synthesis mixture after 3 days.

batch 2 (SiO_2/Al_2O_3 = 10), and the P_c phase followed by P_c + ZSM-5 and finally by ZSM-5 for batch 3 (SiO_2/Al_2O_3 = 8.3)).

For a SiO_2/Al_2O_3 molar ratio of 6 (batch 4), P_c was the initial zeolite phase observed. It transformed in time to the ZSM-5 phase. In contrast to batch 3 (SiO_2/Al_2O_3 = 8.3), P_c remained present even after 16 days of synthesis but the ZSM-5/P_c ratio increased with time. Crystallization curves are presented in Fig. 3.

At a SiO_2/Al_2O_3 molar ratio of 3.5 (batch 5), P_c was the only zeolitic phase observed during the entire crystallization process of 16 days. As seen from Fig. 4, the concentration of P_c passes through a maximum at around 5 days. The decrease in the P_c phase with the synthesis time is expected to be followed by the appearance of a different

TABLE 2

Silica/Alumina Ratios of the Starting Mixtures and of the Final Composite Powders[a]

Batch no.	SiO_2/Al_2O_3 ratio (mol/mol)	
	Starting gel	Final sample
2	10.0	9.4
3	8.3	12.9
4	6.0	11.8
5	3.0	4.3
6	8.3	6.0

[a] Analyzed by the wet analytical method using atomic absorption spectroscopy.

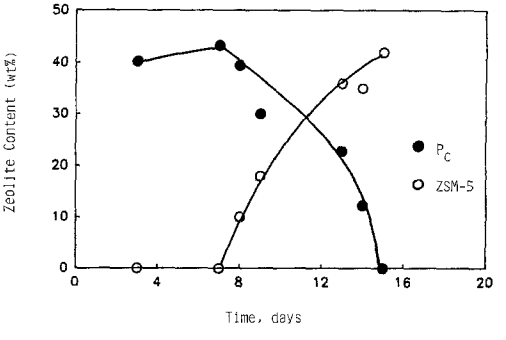

FIG. 1. Change with time of the zeolite content during the synthesis of the composite catalyst in batch 3.

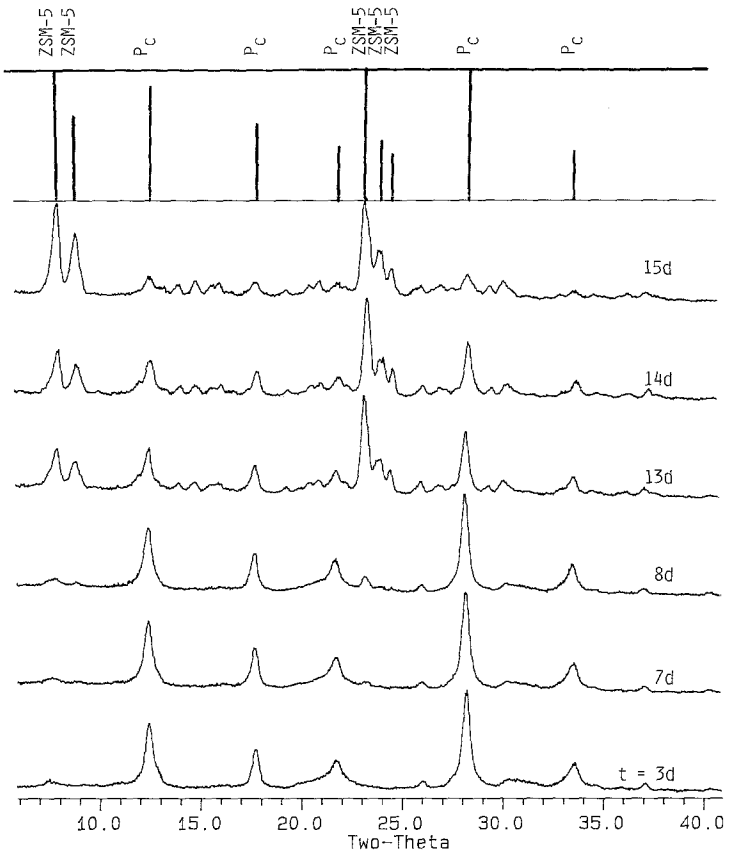

FIG. 2. XRD patterns of the solid samples withdrawn at different time intervals during the synthesis of the composite catalyst in batch 3.

and more stable zeolite phase rather than its conversion to an amorphous phase. However, the XRD patterns have not revealed any new phase. This might be due to the small size of the crystallites formed. As discussed later, IR can detect such clusters. Consequently, in order to confirm such a possibility, some of the samples were examined by IR. The IR spectra of the samples corresponding to 5 (maximum P_c phase) and 10 days (less P_c phase) of synthesis were similar and neither indicated the presence of five-membered ring structures, which are known to be precursors for mordenite and ZSM-5. Hence, it appears that the P_c phase transforms into an amorphous phase with time.

The synthesis conducted without any TPA cations in the gel (batch 6), for a SiO_2/Al_2O_3 molar ratio of 8.3, resulted in the P_c phase as the only crystalline phase even after 15 days. The crystallization curve is also presented in Fig. 4. This experiment clearly indicates that the presence of the organic cation is absolutely necessary for the formation of the ZSM-5 phase, but is not necessary for the formation of the P_c phase. One may note the presence of a maximum in P_c at 10 days. Beyond 10 days the crystallinity decreases because the P_c phase transforms into an amorphous phase.

Recent studies of Katovic *et al.* (*16*) showed that a gel with composition 4.2 Na_2O–Al_2O_3–3.6SiO_2–320H_2O (a composition comparable to that of batch 5 of Table 1) led initially (at a temperature of 80°C) to

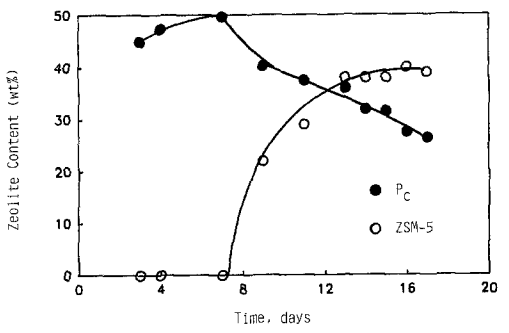

FIG. 3. Change with time of the zeolite during the synthesis of the composite catalyst in batch 4.

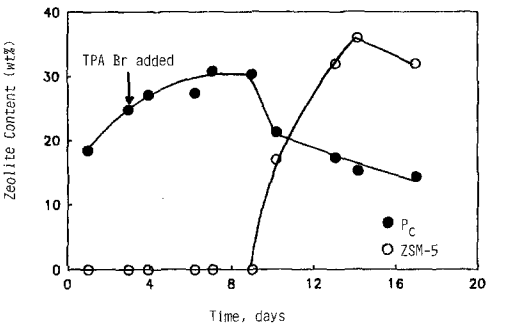

FIG. 5. Change with time of the amount of crystallization during the synthesis of the composite catalyst in batch 7.

the tetragonal form (P_t) of Zeolite P, which, however, completely transformed in time to its cubic form (P_c). In their study, the P_t phase formed after 6 h and completely transformed to the P_c phase after an additional 5 h. The P_t phase was not detected in the present experiments perhaps because the sampling was performed only once per day.

The data from batches 3, 4, and 5 show that the maximum concentration of the P_c phase was reached after 5–6 days of synthesis in the presence of the TPA cation template. However, in its absence (batch 6, Fig. 4), the maximum shifted from 5 to about 10 days. Thus the presence of the TPA^+ species in the gel enhances the rate of formation of the P_c phase apart from inducing the transformation of P_c to the ZSM-5 phase.

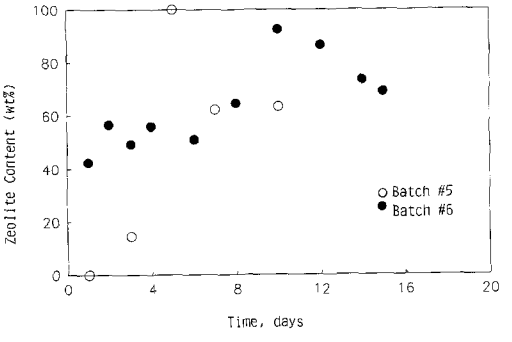

FIG. 4. Change with time of the P_c zeolite content during the synthesis of the composite catalyst in batches 5 and 6.

It is unlikely that the tetrapropyl ammonium cation with a diameter of 8–9 Å (*13*) can be accommodated in the pores of Zeolite P, which has a free aperture size of 3–4 Å (*13*), even though a P-type zeolite that contains tetramethyl ammonium cations has been reported (*18*). Furthermore, the absence of IR stretching frequencies characteristic of the tetrapropyl groups in samples that contained only P_c (e.g., batch 3 before the transformation of P_c to ZSM-5) indicates that TPA cations were not present in composite catalysts comprised of amorphous alumino-silicate and the crystalline P_c phase. On the other hand, a number of studies have indicated that TPA cations constitute templates for the formation of the ZSM-5 framework (*19–21*).

In order to verify whether the TPA cations are necessary from the beginning of the crystallization process for ZSM-5 to be generated, an experiment was conducted during which the organic cation was added after 3 days (batch 7) time at which the P_c phase has been already formed in significant amount. The molar composition of this batch was identical to that of batch 3. A comparison of the crystallization curves of batch 7 (Fig. 5) and of batch 3 (Fig. 1) shows that (i) the time required to reach the maximum concentration of P_c is increased and (ii) the maximum yield of the ZSM-5 phase reflected in the crystallinity of the system

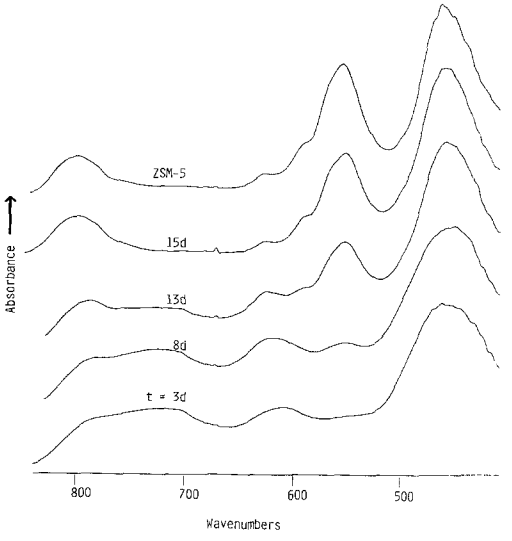

FIG. 6. IR spectra of the composite catalysts, heat treated at 550°C, withdrawn at different times from batch 3.

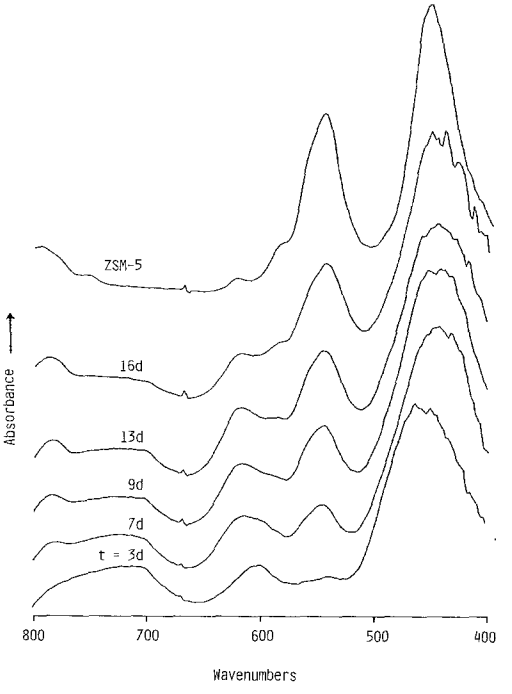

FIG. 7. Infrared spectra of the composite catalysts, heat treated at 550°C, withdrawn at different times from batch 4.

is slightly decreased (within the limits of experimental error), when the addition of the TPA cations is delayed until the end of the third day. On this basis, one can conclude that P_c and ZSM-5 phases are in competition only in the presence of TPA. Due to a small induction period coupled with a high rate of crystallization, the P_c phase forms more rapidly and consequently is more easily detected by XRD. In contrast, the ZSM-5 precursors do not generate nuclei for a long time and are not detectable by XRD (1) but may be detected by IR. For this purpose, the samples of batches 3 and 4 that contain TPA^+ were examined by IR. The IR spectra (800 cm^{-1}–400 cm^{-1}) of these samples together with that of pure ZSM-5 (Mobil, MZ-44) are presented in Figs. 6 (batch 3) and 7 (batch 4), respectively. In Fig. 6, a peak at 550 cm^{-1}, characteristic of the five-membered rings (*22–24*), which are known to be precursors for some zeolitic structures, such as mordenite and pentasil, appears after 8 days with a weak intensity. Its intensity increases, however, with time. The 450 cm^{-1} peak, which is present in all the samples, can be assigned to the Al–O or Si–O linkage (*26*). Furthermore, a shoulder at 1222–1225 cm^{-1} (not shown in the figures) was observed only for the samples for which a well-developed peak at 550 cm^{-1} was also identified. The peak at 1225 cm^{-1}, which is due to the external asymmetric (structure sensitive) stretching vibration, is characteristic of the ZSM-5 (25). Similar trends in IR were also observed for batch 4 (Fig. 7). Every structure (precursors, nuclei, small crystallites undetectable by XRD, and crystallites detectable by XRD) that contains five-membered rings can be detected by IR spectra. The optical density ratio at 550 and 450 cm^{-1} can be taken as a measure of such rings (this ratio is 0.75 for 100% ZSM-5). The results presented in Table 3 compare IR and XRD measurements. It is obvious that the IR values are higher because they account for every five-membered ring structure.

Although at this stage one cannot explain

TABLE 3

IR Detectable Structures and XRD Crystallinity

	IR detectable structures[a]	XRD crystallinity
Pure ZSM-5 (mobile, MZ-44)	100%	100%
Batch 3		
t = 3d	—	—
7d	—	—
13d	44%	35%
15d	73%	42%
Batch 4		
t = 3d	—	—
4d	—	—
7d	19%	—
9d	27%	18%
11d	37%	29%
17d	48%	38%

[a] With respect to pure ZSM-5.

the mechanism by which the P_c phase is transformed into the ZSM-5 phase, a possible scheme is outlined in Table 4. This scheme suggests that (Al, Si)O_4 tetrahedra formed in the gel can form either five-membered rings with an attached tetrahedron (5 − 1) or single four-membered rings (S4R). At the highest SiO_2/Al_2O_3 ratio studied (*10*), the latter do not compete favorably with the former and mordenite results. At the lowest SiO_2/Al_2O_3 ratio or for any SiO_2/Al_2O_3 ratio but in the absence of TPA^+, S4Rs predominate and P_c results. At intermediate SiO_2/Al_2O_3 ratio and in the presence of TPA^+ there is a competition between the S4R and 5 − 1 structures and while the former yield P_c more rapidly, the process is reversible so that in time, ZSM-5 is the final product. Additional evidence in favor of this scheme is provided by the results of chemical analysis presented below.

TABLE 4

Scheme for the Formation of Different Zeolitic Phases

(i) amorphous gel → (Al, Si)O_4 tetrahedra → 5 − 1 or 4 + 6 → mordenite (batches 1 and 2)

(ii) amorphous gel → (Al, Si)O_4 tetrahedra → S4R → P_c (batches 5 and 6)

(iii) amorphous gel → (Al, Si)O_4 tetrahedra ⇌ S4R ⇌ P_c

5 − 1 → ZSM-5

(batches 3, 4, 7)

5 − 1: five ring with an attached tetrahedra
4: four-membered ring
6: six-membered ring
S4R: Single four-membered ring

The chemical analysis (Table 2) shows that the SiO_2/Al_2O_3 molar ratio of the final composite sample is very close to that of the starting gel for batch 2. In batches 5 and 6 the ratios are comparable, but not in as close agreement as for batch 2. For batches 3 and 4, in which the ZSM-5 phase appeared, the final composite samples have SiO_2/Al_2O_3 molar ratios significantly higher than those of the starting gels. In batch 2, mordenite was the only crystalline phase present, the remaining material being the amorphous phase. P_c was the only crystalline phase in both batches 5 and 6. In contrast to mordenite or P_c, the ZSM-5 zeolite (batches 3 and 4) has a very low aluminum content. As P_c is converted into ZSM-5, Al species from the P_c phase must return to the solution, to permit the enrichment in silica needed for the formation of ZSM-5. This Al is apparently not incorporated into the amorphous phase. These results, in conjunction with the observation that the P_c phase is free of the TPA cation, suggest that the P_c phase transforms into ZSM-5 by first "redissolving" followed by a template-stimulated nucleation crystallization.

The ideal unit cell composition of mordenite is $Na_8[(AlO_2)_8(SiO_2)_{40}]\ 24H_2O$. In reality, it can have a silica/alumina molar ratio between 8.3 and 10 (*27*). In batches 1 and 2 (see Table 1), the starting gels have a SiO_2/Al_2O_3 molar ratio of 10 and this appears to be an appropriate composition for the formation of mordenite. The induction period in these batches was long (9–12 days), but this is due mainly to the low temperature used. Elsewhere (*10*) it has been noted that mordenite is the initial phase that is formed, followed closely by ZSM-5; they transform

later into the analcime phase. In a different study (*28*), the ZSM-5 phase was found to form initially, followed by its transformation to mordenite; after a long time, both phases transform into α-quartz. The gel compositions and the synthesis temperatures employed in Refs. (*10, 28*) were different from each other and also from those employed in the present study. In the present work, only the mordenite phase was detected in batches 1 and 2 after 16 days.

Zeolite P has the following ideal unit cell composition: $Na_6[(AlO_2)_6\ (SiO_2)_{10}]\ 15\ H_2O$. In real synthesized samples the silica/alumina ratio varies between 2.2 and 5 (*18*). For this reason, the P phase is expected to form easily in batches 3–6. Because Zeolite P has more Al atoms per unit cell (6 out of 16 tetrahedral atoms), the relatively high repulsive forces between the charged aluminum atoms make the lattice metastable. In contrast, the Zeolite ZSM-5 has at most 8 Al atoms in a total of 96 tetrahedral atoms per unit cell (*29*), and for this reason it is more stable than the P_c phase. Hence, the formation of ZSM-5 phase at the expense of the P_c phase observed in batches 3 and 4 appears to be in qualitative agreement with the stabilities of different zeolites.

B. Activity and Selectivity in the Conversion of n-hexane

Three CA composite zeolite samples were withdrawn from the gel mixture during the synthesis of batch 3 (Table 1) at the end of 8, 9.5, and 15 days of synthesis and were used as catalysts in the *n*-hexane conversion reaction. From XRD analysis, the above samples were found to contain 10, 20, and 42 wt% ZSM-5 (Fig. 1), respectively. Prior to calcination, the first two of the above three samples contained, in addition to ZSM-5, 38 and 32 wt% P_c. However, during the calcination step (550°C for 24 h), which was necessary to burn off the organic cation, the P_c phase collapsed into an amorphous phase, while there was no measurable change in the amount of ZSM-5. The final composite zeolite, after calcination, NH_4^+ exchange and a final calcination, had only ZSM-5 as the crystalline phase apart from the amorphous silica–alumina. Details regarding all the catalysts used in the reaction studies are given in Table 5.

Table 6 summarizes the kinetic parameters and the rate constants for *n*-hexane cracking over various catalysts. As an example, a typical plot of $-\ln(1 - x)$ vs space time is provided in Fig. 8a, and a typical Arrhenius plot, is shown in Fig. 8b. For all the CA and the CB composite catalysts, the *n*-hexane cracking rate was found to be first-order over the temperature range of 370–490°C. It should be noted that the conversion data were collected during the initial time period in which the deactivation due to coking was low. For the amorphous silica–alumina sample, the deactivation was severe, and hence the activity at 723 K was determined by extrapolating to zero time the conversion versus time plot.

The C_6–C_{10} aromatic selectivity, which reflects the extent of secondary reactions that occur mainly in the ZSM-5 pores, was plotted against the *n*-hexane conversion for various reaction temperatures (Fig. 9). The plots include data from all the catalysts investigated here.

Figure 9 shows that there is some correlation between the selectivity and activity with a scattering that is larger at 380°C and smaller at higher temperatures. A comparison between the *n*-hexane cracking rate constants (last column of Table 6) shows that (i) the 10 wt% CA composite zeolite has an activity comparable to that of the pure zeolite, (ii) among the CA composite zeolites, the rate constant increases nonlinearly with increasing ZSM-5 content, (iii) the CB mechanical mixture composites have activities significantly lower than those of their CA composite counterparts or the pure zeolite, and (iv) among the CB composites the activity increases nonlinearly with increasing ZSM-5 content. The activation energies E_a over a temperature range of about 120 K were mostly between 10 and 13 Kcal/mol and this is approximately the value for the

TABLE 5

Catalysts Used in *n*-Hexane Conversion Reaction

Sample designation	Nominal chemical composition			Average ZSM-5 crystallite size (from SEM) (μm)	Method of preparation
	Amorphous phase	Zeolite phase			
	Alumina content (wt%) (by chemical analysis of total sample)	Zeolite content (wt%) (from XRD)	SiO_2/Al_2O_3 ratio (mol/mol) (from EDX)		
(a) Composite zeolite samples (CA)					Present study (from batch 3; Table 1 and Fig. 1)
10% Composite	N.D.	10	20	2	
20% Composite	N.D.	20	22	3	
42% Composite	15	42	22	3	
(b) Mechanical mixtures (CB)					As in Ref. (*15*)
10% Mechanical	15	10	30	5	
20% Mechanical	15	20	30	5	
42% Mechanical	15	42	30	5	
(c) Pure zeolite sample	—	100	30	5	As in Ref. (*14*) for different SiO_2/Al_2O_3 ratios

Note. nd, not determined.

TABLE 6

Kinetic Parameters and Rate Constants for *n*-Hexane Conversion Reaction over Various Catalysts Tested[a]

Catalyst	Kinetic parameters		k at 723 K g h^{-1} (g catalyst)$^{-1}$ (atm)$^{-1}$
	ln k_0 g h^{-1} (g catalyst)$^{-1}$ (atm)$^{-1}$	E_a (kcal/mol)	
(a) CA composites			
10% Zeolite	7.3564	10.1	1.39
20% Zeolite	11.5130	15.7	1.79
42% Zeolite	9.8688	12.6	3.00
(b) CB composites			
10% Zeolite	5.6794	11.6	0.09
20% Zeolite	6.4145	10.0	0.58
42% Zeolite	8.2628	11.8	1.00
(c) Pure zeolite	8.7748	12.2	1.33
(d) Amorphous silica–alumina			0.03[b]

[a] Assuming first-order kinetics $r = k\,P_{n\text{-hexane}}$, where $k = k_0 e^{-E_a/RT}$ and $P_{n\text{-hexane}}$ is the partial pressure of *n*-hexane.

[b] Initial rate constant obtained from conversion versus time-on-stream plot.

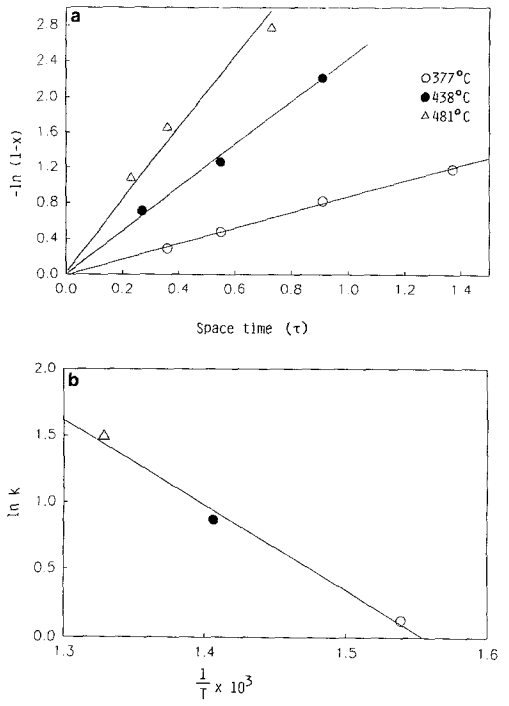

FIG. 8. (a) Conversion plot used to determine rate constants for 42 wt% CA composite. (b) Arrhenius plot for 42 wt% CA composite for *n*-hexane cracking reaction.

pure ZSM-5. This behavior, in conjunction with the observation that the pure silica–alumina sample has a low activity, indicates that the zeolite component of the composite is the locus of the *n*-hexane cracking. Furthermore, from Fig. 9, it is clear that at a given reaction temperature, the C_6–C_{10} aromatic selectivity depends on the extent of *n*-hexane conversion rather than on the nature of the catalyst samples (method of preparation or zeolite content). The hydrogen transfer reaction leading to the formation of aromatics is sensitive to the aluminum content of the ZSM-5 framework (*30*) and also to the pore opening (*30*). As long as these values remain comparable or in a range where their influence is negligible, the aromatic selectivity is expected to depend only on the conversion level. The data presented in Fig. 9 confirm to a large extent such a conclusion.

The observed differences in *n*-hexane cracking activity could arise from either differences in crystallite size and/or the different SiO_2/Al_2O_3 ratios (or acid site density) of the ZSM-5 zeolites present in the composites. SEM indicates that for the pure ZSM-5, the average crystallite size is about 5 μm diameter. This pure ZSM-5 was also used in the preparation of the CB-type composites. For the CA composites, the size of the zeolite particles was in the range of 1–3 μm diameter. For such crystallite sizes, the effectiveness factor for *n*-hexane (diffusion coefficient 3×10^{-4} cm^2 s^{-1}) cracking reaction is essentially unity (*31*). Hence, the measured rate constants for the reaction given in Table 6 are not believed to be influ-

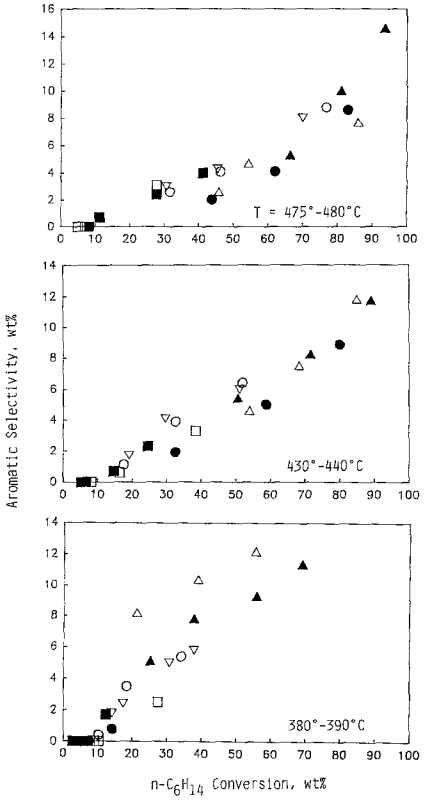

FIG. 9. Variation of aromatic selectivity with *n*-hexane conversion at different reaction temperatures. ○ Pure ZSM-5; ● 10% CA composite; △ 20% CA composite; ▲ 42% CA composite; ■ 10% CB composite; □ 20% CB composite; ▽ 42% CB composite.

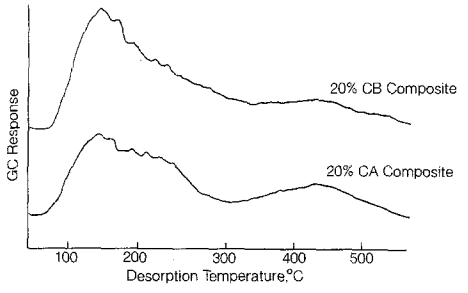

FIG. 10. Ammonia TPD spectra of 20% CA composite and 20% CB composite samples. Conditions: Weight of sample = 0.1 g; NH_3 adsorption temperature = 20°C; heating rate 10°C/min; TC detector attn × 4.

enced by the diffusion in the ZSM-5 particles.

As the *n*-hexane cracking reaction is acid catalyzed and occurs either by monomolecular protolytic cracking (*32*) and /or by carbenium ion formation followed by β-scission (*33*), the presence of strong acid sites is necessary for the primary reaction. The low activity of the amorphous SiO_2/Al_2O_3 sample indicates that the sites associated with the tetrahedral Al cations on the amorphous silica–alumina surface are less active in causing the primary reaction. Thus it becomes necessary to assess the intrazeolitic sites that have a high intrinsic site activity (*34*) both in the CA and CB samples. The SiO_2/Al_2O_3 ratio of the zeolitic component has been probed via EDX in a SEM. Table 5 shows that the SiO_2/Al_2O_3 molar ratios, measured by EDX, of individual ZSM-5 crystallites present in the CA samples vary from 20 to 22; in the CB samples the molar ratio is about 30. The uncertainty in these values is expected to be large.

Thus the EDX data suggest that the number of Al sites in the ZSM-5 component of the CA catalysts is greater than in the CB catalysts or pure ZSM-5. In other words, the number of acid sites is likely to be greater in the former than in latter catalysts.

The TPD of ammonia was used to probe the difference in acidities. The TPD spectra in Fig. 10 compare the 20% CA catalyst to the 20% CB catalyst, and Fig. 11 similarly compares the 42% catalysts. There is no discernable difference, for 42% zeolite content, in the number or distribution of strong acid sites (desorption above 350°C). For 20% zeolite the CA composite does show a somewhat higher acid concentration above 350°C than the corresponding CB sample. There are subtle differences between 100 and 350°C, where the CB catalysts have a broader distribution and a greater population. This behavior does not explain why the CB catalysts are less active, however.

Perhaps the activity is not solely dependent on the acidity and another cause of a physical nature is responsible for the higher activity of the CA catalysts. A possible explanation is the better connectivity between the two phases that is achieved when the ZSM-5 catalysts are generated via *in situ* crystallization.

CONCLUSIONS

The present investigation shows that ZSM-5-containing composites can be prepared from gels rich in alumina and low in TPA^+ templates in a narrow range of SiO_2/Al_2O_3 molar ratios in the starting gels. A SiO_2/Al_2O_3 molar ratio of 10 led to a composite containing mordenite as the crystalline phase while a molar ratio of 3 led to P_c zeolite. For molar ratios of SiO_2/Al_2O_3 between 8.3 and 6, the phase sequence is amorphous gel → P_c → ZSM-5. When the molar ratio of SiO_2/Al_2O_3 is 8.3, the amount

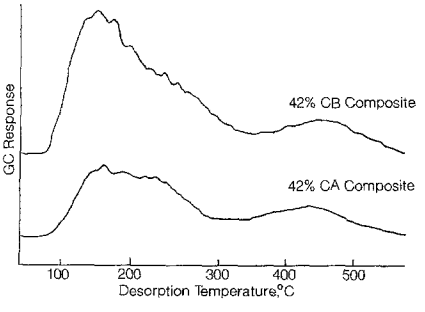

FIG. 11. Ammonia TPD spectra of 42% CA composite and 42% CB composite samples. (Conditions the same as those in Fig. 10.)

of P_c passes through a maximum, and subsequently decreases until, after 15 days, the P_c phase is no longer detected.

From the gels based on initial molar composition of SiO_2/Al_2O_3 = 8.3 and TPA^+/Al_2O_3 = 0.45, samples have been obtained after crystallization *in situ* for 8, 9.5, and 15 days of synthesis. These samples have been calcined at 550°C for 24 h, ammonium ion exchanged, and again calcined at 550°C for 4 h. XRD showed that they have 10, 20, and 42 wt% ZSM-5 zeolite, respectively, the balance being amorphous silica–alumina. For the *n*-hexane cracking reaction, the above samples exhibited activities significantly higher than those of the corresponding (same zeolite content) composite samples prepared by dispersing preformed ZSM-5 zeolite particles in an aluminosilicate gel. A 10 wt% composite prepared by the *in situ* crystallization method exhibited an activity comparable to that of the ZSM-5 zeolite. Although the amounts of strong acid sites as probed via NH_3 desorption were comparable in both types of composites, the *in situ* crystallized composites probably have a better connectivity between the two phases than the catalysts based upon preformed ZSM-5. This may then be the cause for the differences in activity.

REFERENCES

1. Jacobs, P. A., Derouane, E. G., and Weitkamp, J., *J. Chem. Soc. Chem. Commun.* 591 (1981).
2. Ruckenstein, E., *AIChE J.* **16,** 151 (1970).
3. Nandapurkar, P. J., and Ruckenstein, E., *Chem. Eng. Sci.* **39,** 371 (1984).
4. Derouane, E. G., and Gabelica, Z., *J. Solid State Chem.* **64,** 296 (1986).
5. Jacobs, P. A., and Martens, J. A., "Synthesis of High-Silica Aluminosilicate Zeolites." Elsevier, The Netherlands, 1986.
6. Szostak, R., "Principles of Synthesis and Identification." Van Nostrand–Reinhold Catalysis Series, Van Nostrand–Reinhold, New York, 1989.
7. Narita, E., Sato, K., Yatabe, N., and Okabe, T., *Ind. Eng. Chem. Prod. Res. Dev.* **24,** 507 (1985).
8. Shiralkar, V. P., and Clearfield, A., *Zeolites* **9,** 363 (1989).
9. Argauer, R. J., and Landolt, G. R., US Patent 3,702,886 (1972).
10. Erdem, A., and Sand, L. B., *J. Catal.* **60,** 241 (1979).
11. Chao, K-J., Tasi, T. C., and Chen, M. S., *J. Chem. Soc. Faraday Trans. 1* **77,** 547 (1981).
12. Barrer, R. M., "Hydrothermal Chemistry of Zeolites." Academic Press, San Diego, 1982.
13. Breck, D. W., "Zeolite Molecular Sieves." Robert E. Krieger Publishing, Malabar, FL, 1984.
14. Chen, N. Y., Miale, J. N., and Reagan, W. J., US Patent 4,112,056.
15. Yarlagadda, P., Lund, C. R. F., and Ruckenstein, E., *Appl. Catal.* **54,** 139 (1989).
16. Katovic, A., Subotic, B., Smit, T., and Despotovic, L. A., *Zeolites* **9,** 45 (1989).
17. Lok, B. M., Cannan, T. R., and Messina, C. A., *Zeolites* **3,** (1983).
18. Baerlocher, C. H., and Meier, W. M., *Helv. Chim. Acta* **53,** 1285 (1970).
19. Scholle, K. F. M. G. J., Veeman, W. S., Frenken, P., and van der Velden, G. P. M., *Appl. Catal.* **17,** 233 (1985).
20. Dutta, P. K., and Puri, M., *J. Phys. Chem.* **91,** 4329 (1987).
21. Gabelica, Z., Nagy, J. B., Bodart, P., and Nastro, A., *Thermochim. Acta* **93,** 749 (1985).
22. Shukla, D. B., and Pandya, V. P., *J. Chem. Technol. Biotechnol.* **44,** 147 (1989).
23. Jacobs, P. A., Beyer, H. K., and Valyon, J., *Zeolites* **1,** 161 (1981).
24. Coudurier, G., Naccache, C., and Vedrine, J. C., *J. Chem. Soc., Chem. Commun.*, 1413 (1982).
25. Jansen, J. C., van der Gaag, F. J., and Bekkum, H., *Zeolites* **4,** 369 (1982).
26. Flanigen, E. M., Khatami, H., and Szymanski, H. A., *in* "Advances in Chem. Series 101," p. 201, 1971.
27. Bajpai, P. K., *Zeolites* **6,** 2 (1986) [and references therein].
28. Dai, F. Y., Suzuki, M., Takahasi, H., and Saito, Y., *in* "New Developments in Zeolite Science and Technology" (Murakami, Iijima, and Ward, Eds.), p. 233, Elsevier, Amsterdam, 1986.
29. van der Gaag, F. J., Jansen, J. C., and van Bekkum, H., *Appl. Catal.* **17,** 261 (1985).
30. Wielers, A. F. H., vaarKamp, M., and Post, M. F. M., *J. Catal.* **127,** 51 (1991).
31. Haag, W. O., Lago, R. M., and Weisz, P. B., *Discuss. Faraday Chem. Soc.* **72,** 317 (1981).
32. Haag, W. O., and Dessau, R. M., *in* "Proceedings, 8th International Congress on Catalysis, Berlin, 1984," Vol. 2, p. 305. Dechema, Frankfurt-am-Main, 1984.
33. Greensfelder, B. S., Voge, H. H., and Good, G. M., *Ind. Eng. Chem.* **41,** 2573 (1949).
34. Lombardo, E. A., and Hall, W. K., *J. Catal.* **112,** 565 (1988).